https://doi.org/10.2352/AIT.2026.1.1.9

Atmospheric digital plasma array for one-step surface metallization

David Martinet, Christoph Ellert, *Institute of Systems Engineering, HES-SO Valais-Wallis, HES-SO University of Applied Sciences and Arts Western Switzerland, CH-1950 Sion, Switzerland*
Jian-Lin Huang, Grégoire Magnin, Gilbert Gugler, *iPrint, HEIA-FR, HES-SO University of Applied Sciences and Arts Western Switzerland, CH-1700 Fribourg, Switzerland*

Abstract

A two-dimensional microplasma array operating under atmospheric conditions has been developed previously and, in this work, adapted for direct surface metallization. Unlike conventional plasma arrays where all cells ignite simultaneously, this system enables independent ignition and quenching of individual plasma cells "on demand," a unique feature. The plasma head integrates ink injection capillaries and an aerosol generator, enabling one-step deposition of metallic layers, with silver selected as a representative material for decoration and functional coatings. The work focused on improving plasma head stability, deposition resolution, and sustainability through enhanced electronics, optimized gas flow and advanced manufacturing methods such as laser cutting, 3D ceramic printing, and plasma spray coating of copper. Results demonstrate stable operation up to 30 minutes, improved plume length (1.5 mm at 2 slm), and reproducible ignition during injection of the argon-ink aerosol without clogging. Surface metallization was achieved in one step, though further optimization is required to eliminate ink residues and leakage. This technology offers scalable, high-resolution solutions for functional printing, selective coatings, and advanced manufacturing.

Introduction

Nonthermal micro-plasmas at atmospheric pressure, confined to small dimensions (micrometers to millimeters), find broad technological applications [1], and more recently in metallization processes [2-3]. These micro-plasmas offer significant benefits in printing and coating for surface treatment of heat-sensitive materials like polymers, preserving their beneficial bulk properties. The market for such microplasma arrays is vast, encompassing printing and selective coating in packaging, printed electronics, biotechnology, watch industry, additive manufacturing, and direct-to-shape inkjet printing.

Adhesion and wetting between materials and layers are key challenges in these applications, where nonuniformity often plays a critical role. Partial surface modification is desired in various processes like printing, coating, and gluing, particularly for non-graphical inkjet printing. A high-resolution multi-nozzle plasma jet array for microplasma surface treatment is crucial. This enables selective treatment, ensuring good wetting and adhesion without droplet spreading.

The 2D-microplasma array holds potential for commercialization in surface metallization and coatings. Development efforts have increased the stability and operation of an existing setup [4]. Rigorous testing of materials and manufacturing methods have enhanced global plasma performance and verified metallization conditions with different inks. This technology unlocks cost-effective, high-performance functional printing and coating.

The plasma head's versatility enables seamless integration into existing printing and coating solutions. Multi-head configurations support different gases, allowing chemical selectivity of deposited materials. Applications encompass smart materials, 3D electronics, wearable devices, selective coatings, and customized components.

Materials and methods

The improved version of the overall setup is shown in Figure 1(a), with a 2D view on the plasma head (b), including the capillaries for the ink injection. To enable one-step deposition of metallic layers, it is necessary to introduce atomized metallic ink into the plasma generation system, as shown in Figure 1(a). The atomization system employs a piezo mesh-type nebulizer (12 µm median droplet size, maximum viscosity 3.5 cP) and incorporates an ink recirculation and heating unit to reduce ink viscosity when required. A 3D-printed single-stage cascade impactor-based filter is integrated to remove larger droplets, with a cutoff around 10 µm, thereby ensuring clog-free aerosol delivery through the nozzles. The electrical power to ignite and sustain the plasmas "on-demand" in the nozzles is transmitted to the individually powered electrodes via a special electronic circuitry including protecting filters, as described in [4]. In short, a high-voltage DC pulse ignites the plasma in the desired nozzle, on which a superimposed RF sinusoidal power at 13.56 MHz is set by means of a pilotable RF relay. Improvements were made concerning the physical size of the components, like reducing the size of the inductances, filtering the RF which may damage the transformers. This allows to increase the number of holes in the array while reducing the overall volume of the system. Furthermore, the size of the transformers was reduced, and their configurations were set to separate windings instead of concentric windings around the ferrite core, improving their performances. Impedance measurements show that the electrical characteristics of the setup remain unchanged.

The duration of the plasma in each nozzle is determined by the opening of the dedicated relay. The control commands are sent via a Complex Programmable Logic Device (CPLD), on which the different triggering times (ignition pulse, plasma ON, relay opening) and durations can be varied. The desired deposition pattern can be printed by moving a pilotable X-Y translational stage.

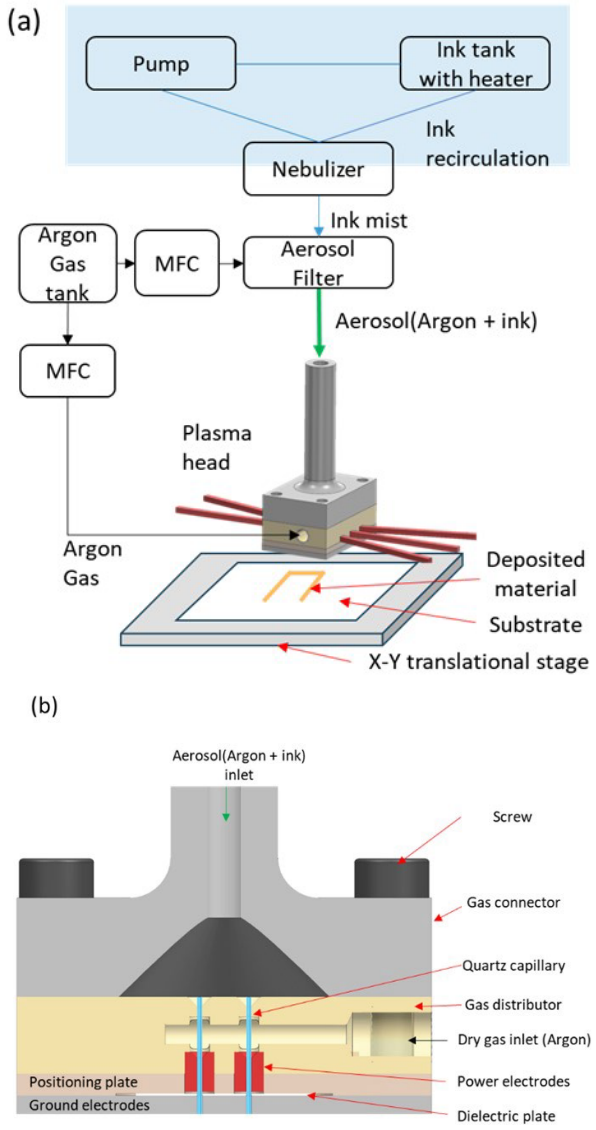

Figure 1. *(a) Schematic of the plasma setup for metallization, including the ink atomization system and plasma head. (b) Cross-sectional view of the plasma head with capillaries for ink injection*

The plasma head consists of multiple functional components fabricated from different materials. Its multilayer structure combined with high resolution and alignment requirements makes precise assembly a significant challenge; therefore, alignment strategies are implemented to ensure accuracy. The design integrates two nozzles of 300 µm in diameter and three 200 µm diameter nozzles to support parametric studies and enable the integration of a dedicated aerosol channel made of quartz and aligned in the center of each nozzle. The latter introduces metallic ink as small droplets in argon (aerosol) into the plasma zone for direct metallization. As illustrated in Figure 1(b), the aerosol is introduced from the top, through the gas connector made of stainless steel, passes through quartz capillaries of 170 and 250 µm outer diameters (100 and 150 µm inner diameters) for the 200 and 300 µm nozzles, respectively, and enters the plasma generation zone. The vertical distance between the capillaries exits and the ground electrode should be varied to investigate the effect of the aerosol presence in the plasma plume or in the intense plasma zone. The metallic gas connector at the entrance ensures electrical ground connection.

The custom-designed gas distributor has two major features. First, it allows argon gas to be inserted into the gap between the hole in the powered electrode and the quartz capillary and thus cooling the outside of the quartz capillaries, and secondly, it holds in place the capillaries centered inside the nozzles and separating the aerosol injection and the plasma gas. The plasma ignites, depending on the experimental conditions and nozzle diameter, around the quartz capillary, and is thus not in direct contact with the metallic ink in the aerosol within the quartz capillary. As the capillary exit is placed downstream of the plasma zone, metallization occurs between the capillary exit and the substrate. This distance can lead to very different treatments of the ink on the surface of the substrate, due to the interaction of the metallic particles in the plasma gas phase and the evaporation of the solvent on the substrate. The gas injected around the quartz capillaries (plasma gas) avoids the metallization of the electrodes and the dielectric plate.

The positioning plate, inserted between the gas distributor and the ground electrodes, see bottom of Figure 1(b), allows alignment of the gas distribution channels, the capillaries, the powered electrodes, the dielectric plate, and the ground electrode. A vertical or horizontal misalignment of each part leads to a reduction of the length of the plasma plume from 1 mm to 0.2 mm, due to gas turbulence in the small gaps created. The thickness of the dielectric alumina plate, ensuring the electric separation of the electrodes, can be varied between 110 and 250 microns to change the ignition voltage and the voltage maintaining the RF plasma. The lower the thickness, the less power is required to sustain the plasma, and therefore the heat dissipated by the plasma will be reduced, increasing the possible operating time of the metallization process. The described configuration offers flexibility to evaluate different strategies, including the introduction of sheath gas via the side dry-gas inlet and the use of dielectric barrier approaches to prevent electrode deposition and clogging.

To reduce the misalignment between the different parts leading to gas turbulence in the plasma nozzle, the plasma head has been redesigned. By plasma spraying copper electrodes directly on the dielectric plate, the number of parts has been reduced. The copper layer deposited on each side of the alumina plate has a thickness of about 10µm, and the thickness of the alumina plate can be reduced to below 100 microns. This PCB-like structure has been characterized with pure argon without aerosol. The fabrication of the thin and thus fragile components requires advanced material techniques, such as 3D laser cutting and plasma spray, which in turn require many iterations to determine suitable manufacturing parameters.

The plasma was characterized by voltage and current time traces on each nozzle, installing a voltage probe (Testec TT–SI 9010) and a current probe (AP015 Lecroy) to measure the total RF-current in all ignited plasma cells (one hole or many holes are ignited). The current and voltage signals are evaluated using an oscilloscope (LeCroy HDO8038A). Electrical impedance of the setup was determined by an impedance analyzer (AdTech ACA-100). During plasma operation, an inline power meter (Impedans Ltd Octive Suite) tracked the RF power sent to the electrodes, prior to the electronic filters (see [4]). Pictures of the plasma were taken with a digital microscope (Dino-Lite AM4113T) to measure the plasma plume length at the exit of the nozzles and the distribution of the plasma inside the nozzle around the capillaries. Images of the metal deposited on the

substrates made from PET and rhodium-coated brass were taken and analyzed by 3D optical and scanning electron microscopes (SEM). The elementary composition of the layer has been determined by energy dispersive X-ray (EDX) analysis, showing the removal of the solvent from the aerosol.

Results

To evaluate the performance of the plasma system for metallization, several deposition and plasma process tests using various settings were conducted. These included adjustments to printing parameters and aerosol control, testing different plasma head designs, and evaluating multiple plasma treatment processes.

Plasma generation is possible whether the quartz capillary fully passes through the assembly or not, as shown in Figure 2 for both nozzle diameters. In Figure 2(a), the quartz capillary extends completely through the assembly and protrudes beyond the ground plate. In contrast, in Figure 2(b), the quartz capillary does not extend fully to the outside of the ground plate. As a result, the plasma plume exhibits a distinctly different appearance in the two configurations. This implies that the length and position of the capillary may have a significant impact on the metallization process. In the 200 µm diameter nozzle, pure argon without aerosol has been injected, and the plasma ignites inside the capillary, whereas in the 300 µm diameter nozzle, the plasma ignites inside and outside of the capillary. However, the resulting plasma plume is shorter compared to the previous design without quartz capillaries. In addition, plasma ignition was observed to occur only 75% of the time across some nozzles, due to misalignment and the added dielectric barrier.

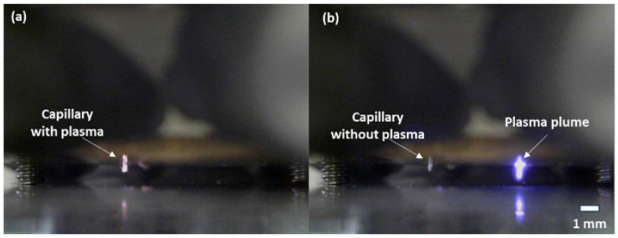

***Figure 2**. Side-view images of the plasma head showing plasma generation for different nozzle diameters with quartz capillaries installed inside the assembly: (a) Plasma ignition with a 200-µm nozzle where the capillary protrudes beyond the ground plate; (b) Plasma ignition with a 300-µm nozzle where the capillary remains inside the nozzle.*

Figure 3 presents the electrical characteristics: (a) voltage and (b) current traces of the plasma for different thickness of the dielectric alumina plate, with and without quartz capillaries, and with the electrodes directly deposited on the alumina plate (PCB-like configuration). The breakdown voltages for the five configurations can be extracted (see inset of Figure 3(a)). One can observe that the breakdown voltage is higher when the powered electrodes are not deposited on the dielectric separation plate, for the same dielectric plate thickness.

In the PCB-like electrodes' configuration, the breakdown voltage increases linearly with the thickness of the dielectric plate. Other thicknesses will be investigated, to confirm the trend. The number of pieces which need to be aligned seem to play a role in the breakdown voltage, as it increases when changing from PCB-like configuration to separated parts (electrodes and dielectric barrier) which all need to be aligned.

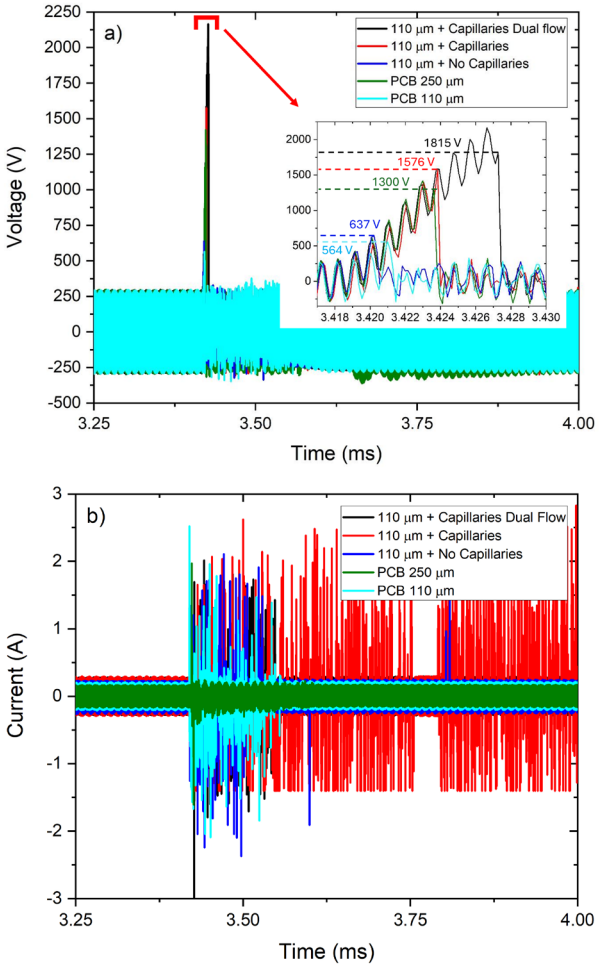

***Figure 3**. RF and DC (a) voltage and (b) current measurements in different plasma head configurations. The higher the thickness or the number of pieces for the same dielectric plate thickness, the higher the voltage needed for the breakdown. The insertion of the quartz capillaries increases the breakdown voltage by a factor of 2. The peak currents at ignition are in the same range, between 2 and 5 A, for all configurations. With 250 µm dielectric thickness, there is only one current spikes, whereas lower thicknesses lead to many current spikes. Gas flow only in capillary leads to many current spikes, due to the presence of the dielectric surface between the electrode and the argon gas.*

Due to insufficient alignment and imperfection of fitting together the small pieces, small gas gaps between the electrode and the dielectric and between the plate and the ground electrode may appear. Theses gas gaps may trap the plasma electrons, which implies that a higher voltage is required to ignite and maintain the plasma. The reduction of the dielectric thickness in both configurations (PCB-like vs assembly) reduces the breakdown voltage, as predicted by the Paschen's law at atmospheric pressure. In addition, we assume that the insertion of capillaries adds a dielectric barrier in the path of the electrons, thus increasing the breakdown voltage event further, as seen in Figure 3(a).

The peak current at the plasma breakdown, at around 3.4ms in Figure 3, varies from 2 to 5 A for all the configurations tested. The larger dielectric thickness exhibits a single current peak at the ignition, whereas all the smallest dielectric thickness configurations show an increased number of current spikes (current peaks of more than 2 A seen in Figure 3(b)), because of the accumulation of local charges on the small distance on the

dielectric plate and quartz (if the capillary is inserted). Charges are stored on the dielectric quartz surface and are released suddenly, creating a small arc (high current in a short period of time). In the case of argon flow only in the capillary, the current spikes are present for a longer time. Whether these arcs occur as well with the injection of ink aerosol needs to be confirmed by further measurements. Moreover, the impact of the arcs for the solvent removal and on the direct metallization step, whether it occurs in the plasma gas phase or on the substrate, will also be investigated.

To assess the performance of the designed plasma head for direct metallization, experiments were conducted using both single-pass and multi-pass printing processes. As a benchmark, we used substrates (PET or Rh-brass) pre-treated with a low-pressure plasma system (Diener ZEPTO) to establish reference conditions for effective silver ink deposition. As pre-treatment, the substrates were placed inside the low-pressure plasma chamber, which was pumped down to 0.2–0.3 mbar before introducing a 30sccm argon flow for plasma generation, increasing the pressure to 1 mbar. The plasma power was set to 150 W, and the substrate surface was activated for 3 minutes under these conditions.

Single-pass process: Simultaneous aerosol deposition and plasma treatment with our atmospheric plasma head, without pre-treatment of the samples with the low-pressure plasma. To increase the deposited layer thickness, the printing operation was repeated up to five times.

Multi-pass process: (1) Pre-treatment of the surface by the low-pressure plasma system, (2) aerosol deposition with 0.01 mm/s printing speed, (3) plasma-assisted reduction of the deposited ink with our atmospheric plasma head with pure argon flow. Steps 2 and 3 were tested both simultaneously and sequentially. To achieve thicker deposited layers, steps 2 and 3 were repeated up to five times.

We compared the performance of two plasma head configurations – with and without the integrated quartz capillary – on the ink reduction on the substrate. The two tested designs differ in aerosol isolation mechanisms: one design electrically isolates the aerosol using a dielectric barrier between electrodes by means of the insertion of the quartz capillary, while the other shields the aerosol only using a sheath gas during its passage near the powered electrodes. Currently, we have limited comparative data on how these two configurations influence metallization efficiency, and the metallization mechanisms with plasma interactions will be investigated in future work.

The multi-pass process generally resulted in the formation of thicker printed films, with thicknesses of 3 to 6 µm, compared with the 0.1 to 0.2 µm layer produced by the single-pass process under the same printing parameters. As shown in Figure 4(a), multi-pass traces not only exhibit a thicker layer but also a wider printed line (approximately 400 µm), which exceeds the nozzle diameter. These results correspond to five repetitions of steps 2 and 3 applied simultaneously. These results may be due to sufficient surface activation, reduced contact angle, and improved wettability. In contrast, the single-pass process yielded thinner layers and narrower printed traces (120 µm) even when the printing was repeated five times, likely due to insufficient surface activation before deposition, as shown in Figure 4(b).

To evaluate the effectiveness of the plasma treatment, we conducted a multi-pass experiment using the plasma head we developed, with pre-treatment also performed by the same plasma head. We found that the distance between the plasma head and the substrate could play an important role in metallization. The printed silver traces are shown in Figure 5. It can be observed that the silver density is lower for a substrate-to-plasma-head distance of 1 mm, as shown in Figure 5(a), compared with Figure 5(b), where the distance is 2 mm. The lower silver density at shorter plasma-to-substrate distances may result from droplet scattering by strong plasma/gas flow, premature solvent evaporation, excessive surface activation or local heating of the substrate, and reduced droplet adhesion or coalescence. Notably, surface deformation of the PET substrate was observed in the plasma-treated regions, as visible in Figure 5.

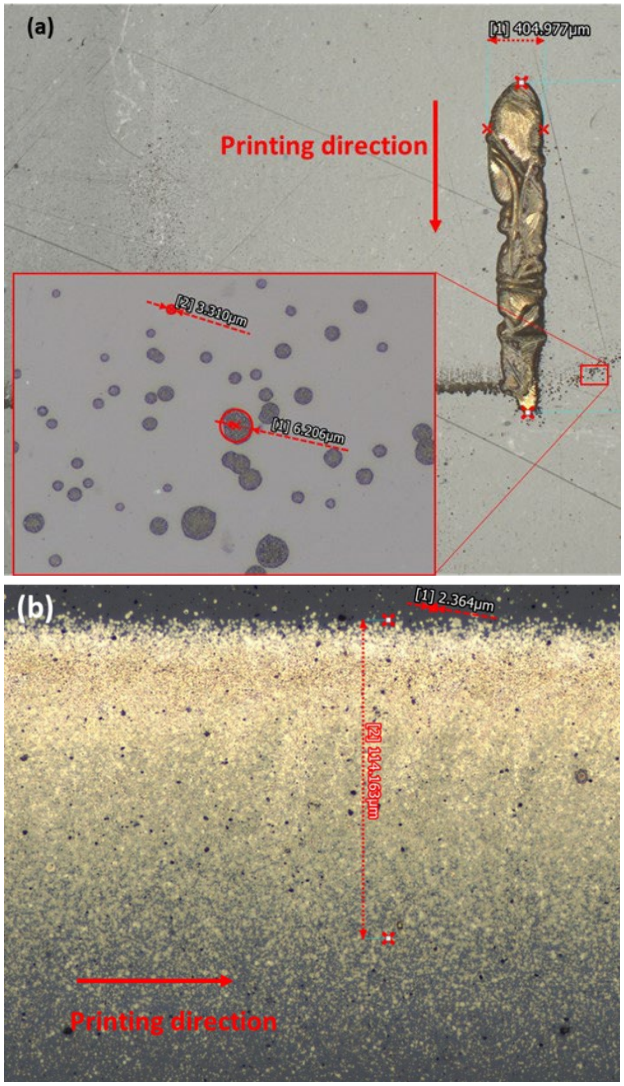

***Figure 4**. Top view of the metallization results: (a) Silver-deposited trace obtained using a multi-pass process with low-pressure plasma pre-treated substrate. The enlarged section highlights droplets printed with higher speed (16.67 mm/s). Due to the higher printing speed, the droplet density is low, and the size of individual aerosol droplets can also be identified. (b) Silver-deposited trace obtained using a single-pass process. The upper part of the image, where the droplet density is higher, corresponds to the region where the nozzle passed during printing.*

In the single-pass tests (Figure 4(b)), deposition and plasma treatment parameters are interdependent and must be optimized concurrently. In contrast, the multi-pass approach allows these parameters to be tuned independently, providing better control and potential for optimization. Further testing is necessary to determine optimal control parameters for consistent

metallization quality. Nevertheless, these early results show that a direct metallization using our plasma system is possible.

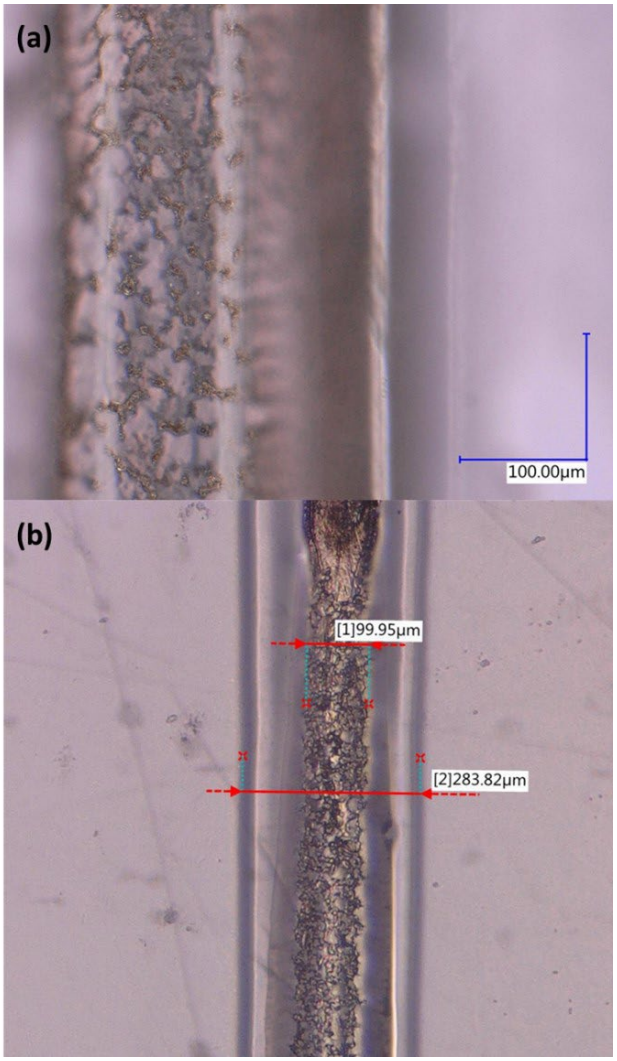

Figure 5. *Silver traces printed by multi-pass metallization process using our developed plasma head. (a) Substrate-to-plasma-head distance of 1 mm, and (b) distance of 2 mm. The substrate is deformed by the plasma treatment, and the density of particles is higher with a larger distance.*

The SEM and EDX analysis in Figure 6(a), reveal that the darker agglomerate contains Ag as the dominant element (53.5 wt%), with a significant oxygen contribution (32.7 wt%), suggesting the presence of silver–oxide–rich domains, possibly due to incomplete removal of organic solvent during the reduction process. At this stage, it remains unclear whether the ink reduction primarily occurs while the aerosol passes through the plasma generation zone or later, when it is deposited onto the substrate, or whether both processes occur simultaneously. Recent studies on plasma-assisted metallization [5] discuss whether reduction happens in flight (aerosol–plasma interaction) or post-deposition; however, in many cases, the exact mechanism is still under investigation. In Figure 6(b), the brighter agglomerate exhibits a lower Ag and O content by nearly a factor of two (32.5 wt% and 18.4 wt%, respectively), with 3 to 4 fold higher contributions from Ni and Rh, which indicates an about three times thinner deposited layer, as the composition of the underlying substrate shines through the silver layer.

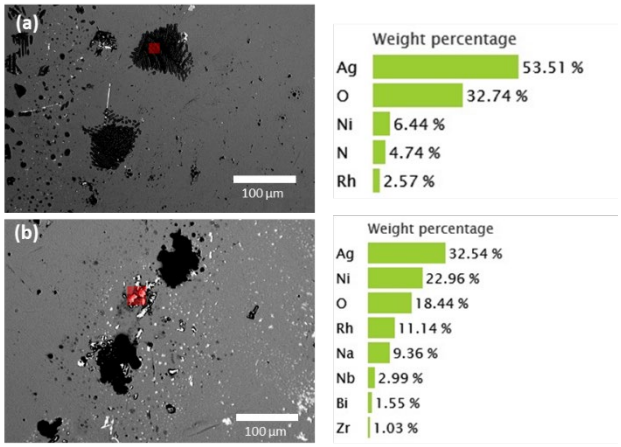

Figure 6. *SEM–EDX analysis of plasma-deposited silver ink on a rhodium-coated brass substrate. SEM images show selected regions (red squares) with corresponding EDX quantification. Both (a) and (b) are taken from the same sample but at different locations following a single-pass metallization process with our plasma head. The deposited ink exhibits distinct visual differences: (a) an agglomerated region with a darker appearance, and (b) a region with a brighter appearance.*

Conclusion

Electrical characterisation of the adapted plasma head allowed to ensure robust ignition and maintaining the “on demand” feature with a time resolution better than 100 milliseconds, besides finding new ways of manufacturing to reduce the costs and improve the mechanical stability. Impedance, power, voltage and current were tracked along the power chain from RF-generator to the plasma head to reduce the power losses. The reduction in size of the electronic components allowed to compactify the overall setup and multiply the number of cells without taking too much space. In particular, the transformer windings and core layout increase the voltage range covered, allowing to insert the dielectric capillaries used to inject ink into the plasma zone without lowering the probability of plasma ignition. More characterisation will be done on the breakdown voltage with the addition of aerosol in the capillaries.

Concerning the metallization process, a custom-designed atomization system was used to create droplets of metallic ink, which was injected into the plasma head using argon as carrier gas (aerosol). The ink was deposited on insulating and conducting substrates and characterized with SEM, 3D optical microscope (length, width, thickness), and with EDX to track the potential impurities in the deposited ink, evaporated ink and the remaining metallic layer. The future parameterized study will consider not only plasma power, but also gas flow rate, atomization conditions, and flow path design, as these factors have a critical influence on substrate treatment and the ink reduction process.

The uniqueness of our digital plasma approach lies in the fact that each of the multiple individual plasma cells in our array can be individually addressed to be ignited and extinguished “on demand”. This individual ignition permits to switch on and off the plasma while the substrate is moving underneath. The multiplexing system to distribute the ignition and the quenching pulses and to maintain plasma power in ignited cells are special developments which are to our knowledge and according to the European patent office so far, the first of its kind worldwide. Aerosol injection into a plasma is not new, but at such low dimensions and in an array of several cells has not been seen in

literature. This design enables the on-demand deposition of metallic layers using a multi-nozzle atmospheric plasma system, a capability that has likewise not been realized previously.

In the future, the design of the PCB-like plasma head using new manufacturing methods (laser cutting and drilling, plasma copper deposition, 3D ceramic printing) will be improved and the injection of the argon-ink aerosol added. The manufacturing methods allow tighter tolerances and will reduce the horizontal and vertical misalignments. The new mechanical design will further improve the mechanical and plasma stabilities and the resolution of the metal layer deposition. Parametrized studies will be performed to find good deposition parameters, depending on the desired resulting layers.

References

[1] Schoenbach, Karl H., and Kurt Becker. "20 years of microplasma research: a status report." The European Physical Journal D 70.2 (2016): 29.

[2] Yamashita, Yu, Shinya Sakuma, and Yoko Yamanishi. "On-demand metallization system using micro-plasma bubbles." Micromachines 13.8 (2022): 1312.

[3] Shchitsyn, Yu D., et al. "Plasma Metallization for Additive Manufacturing of Workpieces Made of 308 LSi Steel." Russian Engineering Research 44.7 (2024): 1005-1010.

[4] D. Martinet, S. Filliger, A. Germanier, G. Gugler, C. Ellert, Plasma. Process. Polym. (2022), e2200131.

[5] Du Y, Yang J, Song K, Jiang Q, Bappy MO, Zhu Y, Go DB, Zhang Y. *Small (2025)*, *21*(11), 2409751.

Authors Biography

David Martinet received the Ph.D. degree in plasma physics from the Swiss Plasma Center (SPC), Ecole Polytechnique Fédérale de Lausanne (EPFL), Lausanne, Switzerland, in 2014. Since then, he has been working as a Senior Academic Associate UAS in the Institute of Systems Engineering, University of Applied Sciences Western Switzerland Valais (HES-SO Valais-Wallis), Sion, Switzerland. His current research interests include mainly atmospheric plasmas for surface treatment, plastic plasmolysis and microbial deactivation, numerical simulations of plasmas and power-to-gas systems for H_2 and CH_4 formation from renewable energies.

Jian-Lin Huang earned his Ph.D. in Microsystems and Microelectronics from EPFL (Switzerland) in 2021. His doctoral work focused on developing interactive robotic and mechanical systems based on smart materials, additive manufacturing, and origami-inspired engineering to overcome the limitations of conventional robotics. He is currently working with iPrint, HEIA-FR, HES-SO University of Applied Sciences and Arts Western Switzerland, where his research focuses on novel inkjet printhead and plasma jet head design, modeling, and the integration of additive and subtractive microfabrication technologies for advanced system development.